simulated studies of particle translocation, aimed at determining the optimum system for analyzing virus particles using this method.

**3286-Pos Board B391**

**Electrical Cellular Interface by Nanoelectrodes**

**Chong Xie**, Lindsey Hanson, Carter Lin, Yi Cui, Bianxiao Cui.

Interfacing cells with micro- and nano-electronic devices has been intensively studied over the last decade. However, a long-term and efficient electrical cell interface is yet to be accomplished. Here we report that vertically aligned nanoscale electrode arrays, which promote tight attachment to cell membrane, form good electrical coupling with cultured cardiomyocytes and neuron cells. Scanning electron microscopy (SEM) analysis shows that cells readily engulf nanoelectrodes by wrapping around them. The tight junction between cells and nanoelectrodes enables high quality and long-term electrical cell interface, which allows us to achieve non-destructive action potential recording with intercellular-like signal quality.

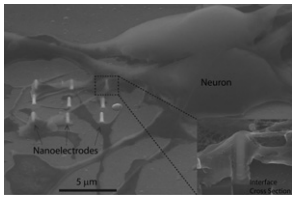


**3287-Pos Board B392**

**Near Field Detection of Beta-Amyloid Proteins by the use of Olfactory Cells and Nano Particles in a Microfluidic Channel**

**Hee-Kyeong Sung**, Jong-Il Ju, Chang-bum Kim, Jung-Dae Suh, Kwan-Soo Kim, Chul-Ju Chae, Hyo-Bong Hong, Ki-Bong Song.

It is well known that Alzheimer's disease (AD) is pathologically defined by the presence of amyloid-beta plaques and neurofibrillary tangles within the brain by advanced medical imaging technique such as computed tomography or magnetic resonance imaging. Currently, in AD-related olfactory sensory loss studies, early olfactory perceptual loss is likely contributed by nonfibrillar, versus fibrillar, amyloid-beta related mechanism in the olfactory system and nonfibrillar amyloid beta deposition is observed within the olfactory bulb. Therefore, the results of the olfactory dysfunction studies represents that if the amount of nano-sized amyloid beta proteins (nano-Abs) is quantified in *in vivo* olfactory system, *in vivo* early diagnosis of AD is possible. In this paper, we have measured the amount of nano-Abs by the use of olfactory cells and nano particles (100nm bead) in a micro-fluidic channel. For sample preparation, nanoparticles are sequentially conjugated with linkers (biotin, straptavidin and so on) and the particles are absorbed (or adhere) into *in vivo* olfactory system. The amount of the conjugated nano-Abs is measured by evanescent field-nano particle coupling effect where we use micro-fluidic channels. As results, in the *in vivo* olfactory system, the coupled optical power with single nanoparticle is around 1nW. The results of quantification with amyloid-related nano-particles in *in vivo* olfactory system will be briefly introduced.

**3288-Pos Board B393**

**The Mechanisms of Decreasing Voltage-Gated Sodium Current by Nanosecond Electric Pulses**

**Vasyl Nesin**.

The application of high-voltage nanosecond electric pulses (nsEP) causes the formation of nanopores in plasma membrane of mammalian cells, modifies function of voltage-gated ion channels. However, it is not known if nsEPs affect ion channels directly, or these effects are mediated in alternate method. We used the whole-cell patch-clamp technique to explore the effect of 300-nsEP on voltage-gated sodium current (INa) in NG108 neuroblastoma cells. Our data have shown that a single nsEP decreased the INa in dose-dependent manners; in parallel nsEP exposures induced a non-inactivating, voltage-sensitive inward current due to nanopore formation. At the same time, the recovery of INa after nsEP exposure took significantly longer than nanopore resealing. To check if the inflow of Na+ through nanopores was efficient enough to overcome the buffering capacity of the pipette, we measured changes of Na+ concentration in ''patched'' cells using the Na+-sensitive fluorescent dye (Sodium Green). These experiments showed that opening of nanopores increases the Na+ concentration in patched cells; however, the maximum increase the Na+ content, even with the most intense exposure (5.3 kV/cm), was only 2.7mM, which could unlikely cause INa inhibition. The measurement of submembrane fluorescence intensity of Sodium Green by nsEP didn't show significant increase of submembrane Na+ concentration too. The another potential pathway of reducing the INa is increasing the intracellular Ca2+ concentration after nsEP and Ca2+ mediated inhibition of INa. Our data showed that nsEP exposure in presence of high concentration Ca2+ buffer - BAPTA (20mM) in the intracellular solution caused reduce INa in NG108 cells. Our finding suggest that decreasing of INa by nsEP was not resulted of inward Na+ leakage through nanopores, as well as Ca2+ release from intracellular stores after nsEP exposure.

**3289-Pos Board B394**

**High Resolution Single Molecule Analysis using Nanopore Recording on Microelectrode Cavity Arrays**

**Gerhard Baaken**, Srujan K. Dondapati, Norbert Ankri, Jürgen Rühe, Jan C. Behrends.

Single molecule detection using biological nanopores in lipid bilayers is crucially limited by noise and bandwidth of the recording. We have tested a newly developed 16-channel microelectrode cavity array (MECA, Ref. 1) for single molecule detection using alpha-Hemolysin (alphaHL) nanopores. The device is based on subpicoliter cavities in a high-quality dielectric polymer adding less than 0.5 pF to the input capacitance of the amplifier (Axopach200B), thereby optimizing noise and bandwidth.

An example trace is shown in Fig.1A with an open state rms noise of 0.65pA at 0-5 kHz. Note that for the blocked state, there is no significant difference between an all points histogram of a 5 kHz filtered trace (black) and that of a event amplitudes defined by averaging (grey). Fig.1B shows 35 single PEG induced blockages superimposed and aligned in time. They are detected as square pulses down to durations<100μs and longer events seem to correlate with deeper blocks. The recording performance of MECAs with high integration densities and superior mechanical stability is expected to greatly facilitate single molecule nanopore analysis in the future.

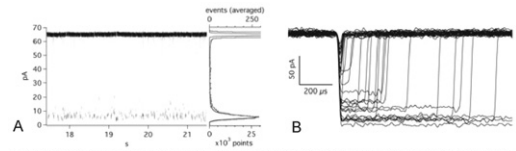


**Fig.1. (A)** Current trace of PEG induced blockages in a single HL pore **(B)** Single superimposed PEG blockages of a HL pore.

(1)Baaken et al.(2008),Lab Chip 8(6):938-44.

**3290-Pos Board B395**

**Biophysical Properties of DNA Strands Attached Inside Single Nanopores**

**Gael H. Nguyen**, Stefan Howorka, Zuzanna Siwy.

Single nanopores attract scientific interest as they serve as a basis for biosensors as well as a system to study interactions and behavior of molecules in a confined space. Nanopores with a particular geometry and surface chemistry can lead to devices that control the transport of ions and molecules in a solution. Here we present a new strategy for ionic and molecular control that is based on attaching single stranded DNA to the inside of a pore wall. The DNA attachment is restricted to the region next to the 10 nm wide small opening of a conical polymer pore. We find that the pore blockade caused by the DNA increases with lower ionic strengths of the electrolyte medium. The result can be explained by the distinct conformations of DNA at different concentrations of electrolyte solution. At low KCl concentrations (10 mM KCl) the DNA is expected to be extended and rigid and causes a greater blockade than the condensed strands at high ionic concentrations. In the future, the ability to tune the opening diameter of DNA-modified nanopores by experimental conditions may be applied to regulate transport of neutral species.

**3291-Pos Board B396**

**Automated Lipid Bilayer Formation Facilitated by Solvent Extraction**

You-Hyo Baek, Joongjin Park, Seunghwan Jeong, Wonyoung Kim, **Tae-Joon Jeon**.

Artificially created lipid bilayers(BLMs) play very important roles in ion channel studies and screening platforms, as well as biosensing applications. Although many applications with lipid bilayer platforms have been suggested, lipid bilayer formation is still based on conventional techniques invented by Montal and Mueller in 1960s. The creation of lipid bilayer membranes is labor intensive, often requiring expertise. The difficulties of lipid bilayer formation preclude a number of useful applications. In the work by Jeon, et al. (Lab Chip, 2008), a frozen membrane precursor was devised and a lipid bilayer membrane was spontaneously created when it was thawed. The frozen membrane precursor can be transported to any place and thawed when a membrane is needed, widening usability of lipid bilayer platforms. However, the film used in this work is a hydrophobic sheet, typically used in the conventional methods. Since membrane formation process driven by spontaneous assembly was unchanged, time required for membrane formation varied with a range of ~30 minutes to 24 hours. To ameliorate the variation of membrane formation time, other work using pin tools was conducted, significantly reducing the formation time by minimizing the solvent volume deposited on the aperture. Taking advantages of previously proposed platforms, we used a thin film made of Polydimethylsiloxane(PDMS) instead of using conventional films. PDMS absorbs organic solvent, thereby the thin film absorbs an excess solvent and

decreases thinning out time, keeping thinning out time more consistent (~30min). Lipid solution was deposited in a small aperture fabricated on a PDMS film and was frozen before use. Upon thawing a lipid bilayer is spontaneously reconstructed with the mean formation time of ~30 min with high success rate (>80%). We also show potential applications with lipid bilayers created in a PDMS film due to its versatility

**3292-Pos Board B397**
**Noise Properties of Ion Current in Rectifying Nanopores**
**Matthew Powell**, Ken Healy, Matt Davenport, Sa Niya, Lane Baker, Sonia Letant, Zuzanna Siwy.
Studying noise properties of ion currents in nanopores can improve detection limits for nanopore sensors as well as give insight into behavior of transport at the nanoscale. We focused on the 1/f⊥alpha noise that is observed in the low frequency regime of the ion current power spectra with the exponent alpha~1. We found that 1/f noise in single conically shaped nanopores in polymer films and glass nanopipettes exhibits asymmetric noise properties with respect to voltage polarity which are not observed for cylindrical and silicon nitride nanopores. The noise asymmetry is shown by the normalized power spectra, which present the noise amplitude at a given frequency, typically 1 Hz for these measurements, divided by the ion current squared. The conically shaped structures rectify the ion current and the currents for the forward bias exhibit noise that increases with voltage in an exponential manner, and are weakly KCl concentration dependent. The normalized noise of currents in the reverse bias is typically voltage-independent but increases with the increase of KCl concentration. The difference in noise properties of the currents is most pronounced when the pore diameter is comparable to the thickness of the electrical double-layer. We discuss two models, which could explain the observed effects: (i) presence of air bubbles, and (ii) crowding of ions at the pore entrance.

## Fluorescence Spectroscopy III

**3293-Pos Board B398**
**Tryptophan Fluorescence from G. Weber to the Present**
**Ludwig Brand**.
Gregorio Weber (Symposium on Light and Life, W.D. McElroy and Glass, B. Eds., 1961) described the fluorescence of tryptophan in proteins. Since that time more than 12,000 papers have appeared related to tryptophan fluorescence. It is used to measure the folding of proteins and the interaction of proteins with each other, with nucleic acids, membranes and small molecules. Time-resolved fluorescence studies have revealed details regarding the excited-state of tryptophan in proteins. Ground-state and excited-state heterogeneity influence the fluorescence and its relation to protein conformation. Excited-state electron transfer, proton transfer, energy transfer, solvent and protein relaxation are among the processes that have been implicated in tryptophan fluorescence in proteins The availability of new experimental, computational and theoretical methods suggest that there are now opportunities for using tryptophan fluorescence for probing protein structure and dynamics. Femtosecond time-resolved techniques and molecular dynamics computations have been of particular value and should provide new information about folded and unfolded structural regions in proteins.

**3294-Pos Board B399**
**Protein Hydration and Coulpled Water-Protein Fluctuations Probed by Tryptophan**
**Dongping Zhong**.
Using tryptophan with site-directed mutagenesis, we can map out global hydration dynamics and water-protein fluctuations with femtosecond resolutions. We clearly demonstrated that tryptopahn is a powerful optical probe to study protein hydration.

**3295-Pos Board B400**
**TDSS in Trp Fluorescence Reveals Multiple Protein and Solvent Relaxation Modes**
**Dmitri Toptygin**, Thomas B. Woolf, Ludwig Brand.
The Time-Dependent Spectral Shifts (TDSS) in the fluorescence of solvatochromic dyes in polar solvents report solvent relaxation dynamics, which in water occurs on the femtosecond timescale. The TDSS in the emission of tryptophan and other solvatochomic fluorophores in proteins span a range of timescales from femtoseconds to nanoseconds. MD simulations of the GB1 protein in TIP3P water made it possible to separate five relaxation modes and to explain their physical origins. Two of these relaxation modes also contribute to the TDSS of dyes in polar solvents.
The ultrafast relaxation mode ($\tau$~35fs) is due in part to the librational relaxation of water molecules and in part to the small adjustments in the local protein structure. This mode is responsible for about half of the total TDSS amplitude. Two collective rotational relaxation modes of water molecules are known. The longitudinal ($\tau_L$~550fs) mode contributes to the TDSS of both dyes in water and tryptophan residues in proteins. The transverse ($\tau_D$~8.3ps) relaxation cannot contribute to the TDSS of dyes in water, but it contributes to the TDSS in proteins having internal water channels or pockets. This can be used to study internal water. In MD simulations using TIP3P water both $\tau_L$ and $\tau_D$ are ~30% shorter than the experimental values.
A small (<0.25Å) adjustment of the GB1 tertiary structure occurs in MD simulations on the time scale of 130ps and results in a 140cm$^{-1}$ contribution to the TDSS. A shift in the sidechain conformation of Glu-42 in close proximity to the fluorophore (Trp-43) is the main contributor to the slow TDSS amplitude (470cm$^{-1}$). This conformational change takes 2.6ns in MD simulations and only 80ps in the experiment, which reveals that in CHARMM22 the potential barriers separating sidechain conformations are too high.

**3296-Pos Board B401**
**Nonradiative Processes in Constrained Trps and Model Compounds**
**Mary D. Barkley**.
Constrained derivatives and model compounds were used to elucidate the nonradiative decay pathways of Trp. Fluorescence quenching by electron transfer from the excited indole to the amide backbone was studied in 7 cyclic hexapeptides.

**3297-Pos Board B402**
**5-Fluorotryptophan as Fluorescent Probe to Characterize an Oligomeric Membrane Protein**
**Jaap Broos**.
The mannitol transporter from *E. coli*, EII$^{mtl}$, belongs to a class of membrane proteins coupling the transport of substrates with their chemical modification. EII$^{mtl}$ is functional as a homodimer and it harbors one high-affinity mannitol binding site in the membrane-embedded C domain (IIC$^{mtl}$). To localize this binding site, single Trp containing mutants of EII$^{mtl}$ were mixed with azi-mannitol, a substrate analogue acting as a Förster resonance energy transfer (FRET) acceptor ($R_0$ of 10 Å). Due to the complex fluorescence decay of Trp, we could not establish whether one or both Trp residues showed FRET with azi-mannitol. To overcome this, we took advantage of the homogeneous decay of 5-fluorotryptophan and this analog was biosynthetically incorporated in 19 mutants. Typically, for mutants showing FRET, only one 5-FTrp was involved, while the 5-FTrp from the other monomer was too distant. This proves that the mannitol binding site is asymmetrically positioned in dimeric IIC$^{mtl}$. The FRET results localized the position of the binding site halfway the first transmembrane helix. Combined with available 2D projection maps of IIC$^{mtl}$, it is concluded that a second resting binding site is present in this transporter. This work demonstrates the potential in structural and mechanistic protein research of a donor-acceptor pair with a very short $R_0$, of which the donor shows homogeneous fluorescence decay kinetics.

**3298-Pos Board B403**
**Time Resolved Fluorescence of the Single Tryptophan in R61, a DD-Carboxypeptidase from Streptomyces: Contributions of Dynamics and Heterogeneity**
Abel Jonckheer, Marc De Maeyer, Anton J.W.G. Visser, Nina Visser, Olaf Rolinsky, Jean-Marie Frere, **Yves Engelborghs**.
The fluorescence emission of the single tryptophan (W233) of the mutant protein DD carboxypeptidase from *streptomyces* is characterized by a red edge excitation shift (REES). This phenomenon is an indication for strongly reduced dynamics in the environment of the tryptophan residue, which has a very low accessibility to the solvent. The Stokes shift however, shows an unusual temperature and time dependence. This, together with the fluorescence lifetime analysis, showing three resolvable lifetimes, can be explained by the presence of three rotameric states which can be identified using the Dead End Elimination (DEE) method. The three individual lifetimes increase with increasing emission wavelength. This is interpreted as each individual lifetime being an average lifetime on its own, indicating the presence of restricted protein dynamics within the rotameric states. This is confirmed by time resolved anisotropy measurements, which demonstrate dynamics within the rotamers but not among the rotamers and by maximum entropy analysis producing distributions that shift with the emission wavelengths. The maximum entropy distributions can also be fitted using a gamma-function analysis, again indicating a dynamic component next to a static heterogeneity. Advanced DEE calculations together with MD simulations indicate the existence of two minima (i.e. substates) within one particular rotamer, with frequent transitions. The global picture is that of a protein with a single buried tryptophan showing strongly restricted dynamics within three distinct rotameric states, one of which is further subdivided into two substates, with different emission spectra.